

Physics in Medicine & Biology

VOLUME 33

SUPPLEMENT I

1988



Proceedings of the World Congress on Medical Physics and Biomedical Engineering

AUGUST 6-12, 1988

SAN ANTONIO, TEXAS

15th International Conference on
Medical and Biological Engineering

8th International Conference on
Medical Physics

6th International Conference on
Mechanics in Medicine and Biology

30th Annual Meeting of the American Association
of Physicists in Medicine

41st Annual Conference on Engineering
in Medicine and Biology

34th Annual Meeting of the Division of
Medical and Biological Physics
Canadian Association of Physicists

10th Annual Meeting of the
Canadian College of Physicists in Medicine



Editors: John W. Clark
Alfred R. Smith

Patricia I. Horner
Kathleen Strum

Supplement published with the co-operation of the
International Union for Physical and Engineering Sciences in Medicine

Journal of the International Organization for Medical Physics

BE12-H.23

A NUMERICAL APPROACH TO PROPAGATIONS OF NONLINEAR PULSE WAVES IN ARTERIES S.G. Wu*, Beijing Polytechnic Univ, Beijing, P.R.China, G.C. Lee, and X.S. Ma*, State University of New York, Buffalo, NY

The present paper mainly deals with methods of numerical solutions for the problems of propagations of nonlinear arterial pulse waves. The artery is assumed to be a thin-walled vessel with the small tissue thickness, and its wall is locally orthogonal, anisotropic, elastic and incompressible. In addition, the blood is modeled to be an incompressible Newtonian fluid with the axisymmetrical flow. In this numerical experimentation, the problem of propagations of nonlinear pulse waves in the aorta of a dog is studied, and the calculation is being performed in IBM-4381 computer. The complete numerical results are obtained, they involve solutions of propagations of the following nonlinear pulse waves: pressure, velocities and flowrate of the blood, as well displacements, velocities and stresses of the vessel wall. These results obtained are very useful to explain the mechanism of propagations of pulse waves in arteries.

BE12-I.2

The Acoustic Radiometer Measured Ultrasonic Therapeutic Instrument
Jin Shuwu, Zhejiang University
Hangzhou, China

According to acoustic radiated force theory and Shotton's method, a new type of acoustic radiometer with float tethered chains for measuring output mean sound power from the ultrasonic therapeutic instrumentations and others ultrasonic equipments is developed. The basic principle, construction design, sensitivity calibrated and measured method are described and remarkable advantage of the radiometer is introduced, too. The reflected target with air backing in diameter 6.1cm has the reflected coefficient 99.9%. The vernier gauge and the optical readout system used for measuring displacements by acoustic radiated force. Nine errors of the radiometer is analysed. The measured repeatability error for confidence level 99.7% is better than 2.3%. The sensitivity constant in 0.5-10 Watts measured range is 10.90mm/w.

BE12-I.1

Ultrasono-Tomography Using FM Chirp Pulse Compression Technique,
T.Moriya*, S.Kiryu, H.Matsukawa, T.Fuse,
Y.Tanahashi+, Tokyo Metropol. Univ.,
1-1, Fukazawa 2-Chome, Setagaya-ku,
Tokyo, 158, Japan, +Tohoku Univ.

To improve resolution of ultrasono-tomography and to remove bioeffects due to the peak intensity of the ultrasonic pulse, we devised a scanning system incorporating FM chirp pulse compression technique.

The B-mode images for tissue mimicking phantoms and abdominal B-mode images are obtained using the system and compared with those obtained using the conventional pulse method.

We have found that (1) the images obtained by this method are similar to those obtained by the conventional pulse method, when the center frequency of the chirp signal from the region of interest is the same with the center frequency of the pulse signal from the same region, (2) without changing the transducer, we obtain the B-mode images with higher lateral resolution only by shifting the center frequency of the chirp signal to the higher frequency.

BE12-I.3

Experiments for a new quantitative reflection imaging, Jian-Yu Lu and Yu Wei*,
Dept. of Biomedical Engineering, Nanjing
Institute of Technology, Nanjing, China

A new quantitative reflection imaging method which reconstructs the sound speed distributions of biological soft-tissues using the outline information and the phases of rf echo signals on these outlines provided by commercial B-scanner has been developed by the authors recently*. This paper reports the experiment studies for image reconstructions using the method introduced above. The rf echo signals are acquired from the commercial Japanese B-scanner SSD-256 using the waveform-storage oscilloscope HP-1780B with a sampling rate as high as 30 MHz. An interface between the B-scanner and the oscilloscope was specially designed to eliminate a random waveform shock caused by big time-delay of the waveform from trigger. The signals sampled are transferred to IBM-PC computer using IEEE-488 parallel interface for image reconstructions. Several agar phantoms were prepared and were put into an echoless tanker for experiments. Compared to the images displayed on the screen of the B-scanner, the images reconstructed are more helpful in the understanding of the structures of the test objects.

World Congress on Medical Physics and Biomedical Engineering, August 6-12, 1988

EXPERIMENTS FOR A NEW QUANTITATIVE REFLECTION IMAGING

JIAN-YU LU and YU WEI

Department of Biomedical Engineering
Southeast University, Nanjing, China

I. INTRODUCTION

As well known, the conventional B-scanner can provide the outlines of the internal structures of biological soft tissues, but not the quantitative distribution of acoustical parameters, such as, sound speed, attenuation etc., of the biological soft tissues. A new quantitative reflection imaging (QRI) method was proposed by the authors^[1,2]. Based on the easy-manipulated acoustical wave transmitting/receiving system of the B-scanner, the quantitative images of the sound speed distribution of the biological soft tissues can be obtained with a datum acquisition interface and QRI reconstruction method. In this paper, the experimental studies of the QRI method will be given in detail.

II. THEORETICAL PRELIMINARIES

Assume that the scattering of acoustical wave in the biological soft tissues is governed by the inhomogeneous Helmholtz equation. Using the first-order approximation and the acoustical wave transmitting/receiving geometry of the B-scanner (see Fig.1), a relationship between the Fourier transform of the derivative of the one-dimensional object function on the line along which a focused acoustical pulse wave is propagated, $\tilde{n}'_z(-2k_0)$, and the measured rf (radio-frequency) echo signal returned from the object to be imaged, $P_r(x', -l_0; k_0)$, can be obtained

$$\tilde{n}'_z(-2k_0) = \frac{4\sqrt{2\pi}\exp[-j(k_0 l_0 + 3\pi/4)]}{\sqrt{k_0}} \left[\frac{P_r(x', -l_0; k_0)}{P'(k_0)} \right]$$

where k_0 is the wave number in the medium which surrounds the object; l_0 is the focal length of the acoustical beam of the B-scanner measured from the surface of the probe and $P'(k_0)$ is the Fourier transform of the mechanical-electrical conversion function of the transducer.

For image reconstruction, one will first obtain the high-frequency component of the one-dimensional object function from the equation above directly, then, recover the low-frequency component of the one-dimensional object function from the high-frequency component using the GP (Gerchberg-Papoulis) frequency extrapolation technique and the a priori knowledges that

the outlines of the internal structures of the object and the phases of the rf echo signals returned from these outlines are known. From the complete spectrum, the one-dimensional object function can be reconstructed. With the scanning of the acoustical beam in a cross-section of the object, tomographic image of the sound speed distribution of the object can be obtained.

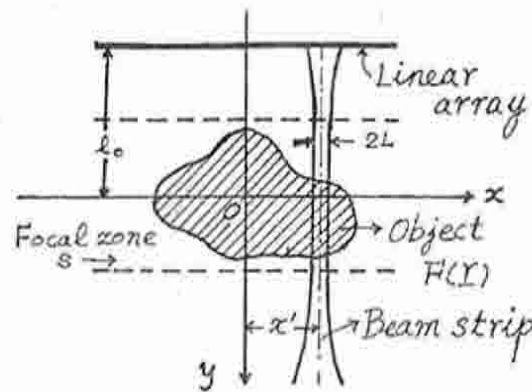


Fig.1 Acoustical wave transmitting/receiving geometry of the B-scanner

III. EXPERIMENTAL SYSTEM

Fig.2 is the block diagram of the experimental system for the QRI method. It consists mainly of five parts and will be described briefly in the following.

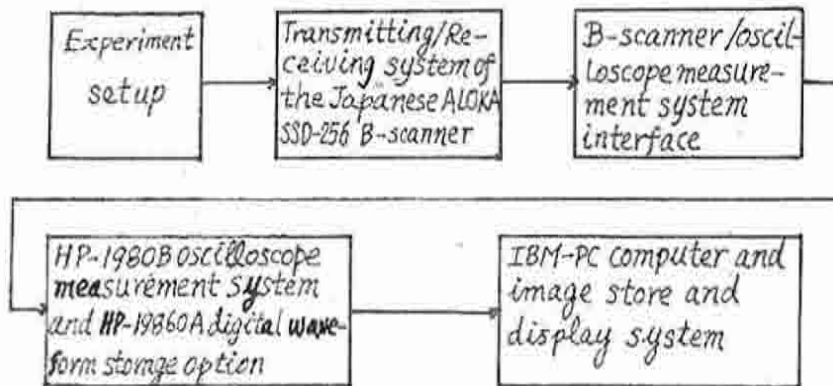


Fig.2 Block diagram of the experimental system for the QRI method

The first part of the experimental system in Fig.2 is the acoustical environment for the datum acquisition of the rf echo signal, as shown in Fig.3.

Fig.4 shows the block diagram of the transmitting/receiving system of the ALOKA SSD-256 B-scanner. It transmits the focused acoustical pulse which can be scanned electrically and receives the rf echo signal returned from the object.

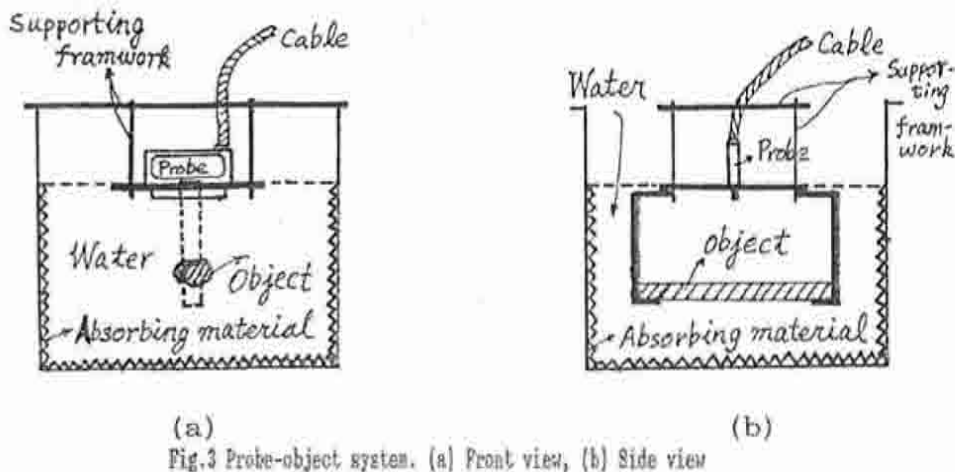


Fig. 3 Probe-object system. (a) Front view, (b) Side view

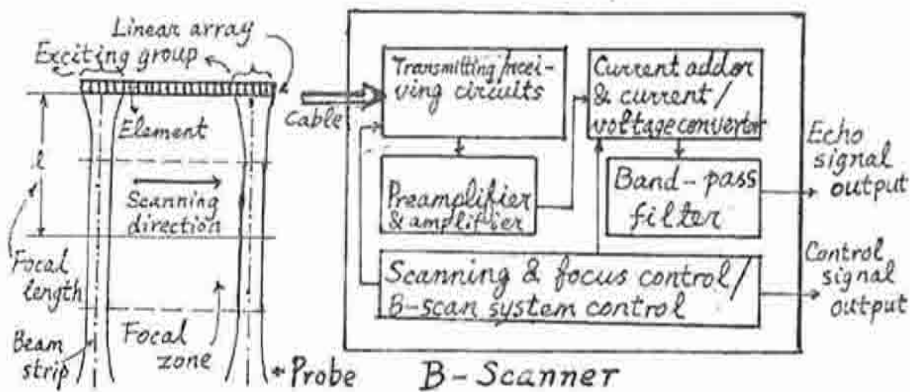


Fig. 4 Block diagram of the transmitting/receiving system of the ALOXA SSD-256 B-scanner

Fig. 5 shows the block diagram of the interface circuit which connects the B-scanner and the oscilloscope measurement system. It is developed by ourselves and is very important for a stable datum acquisition of the rf echo signal in our experiments.

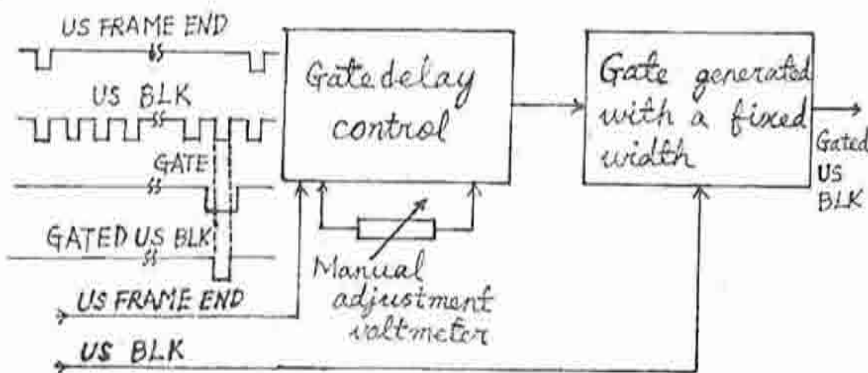


Fig. 5 Block diagram of the interface circuit which connects the B-scanner and the oscilloscope measurement system

The fourth part of the experimental system is the digital waveform storage oscilloscope which is used for the datum acquisition of the rf echo signal. After the echo signal is digitized, the data are transferred to the fifth part, the computer and image system, for image reconstruction and display via the standard IEEE-488 parallel interface.

IV. PREPARATION OF TESTING OBJECTS

In our experiments, the testing objects (phantoms) are prepared with agar powder. First, a wooden model is made by chiselling a square channel of a volume of $20 \times 20 \times 200 \text{ mm}^3$ in the center of a wood and putting glass rods with a length of 200 mm and different diameter into the channel with a desired arrangement. Then, agar aqueous solution is prepared by mixing the agar powder with water and heating it to about 100°C . Finally, the agar phantoms are formed by cooling the heated agar aqueous solution in the wooden model.

Fig.6 shows the cross-sectional figures of three agar phantoms prepared. The phantoms are even in the direction perpendicular to their transversal cross-sections. Fig.6(a) contains six small holes (one of them is of the diameter of 2 mm, and the others are of 3 mm) and is prepared from 4% agar aqueous solution. Fig.6(b) and (c) contain no hole and are prepared from 4% and 8% agar aqueous solution respectively. Fig.7 (a), (b) and (c) are the photographs of these phantoms and are corresponding to Fig.6 (a), (b) and (c) respectively.

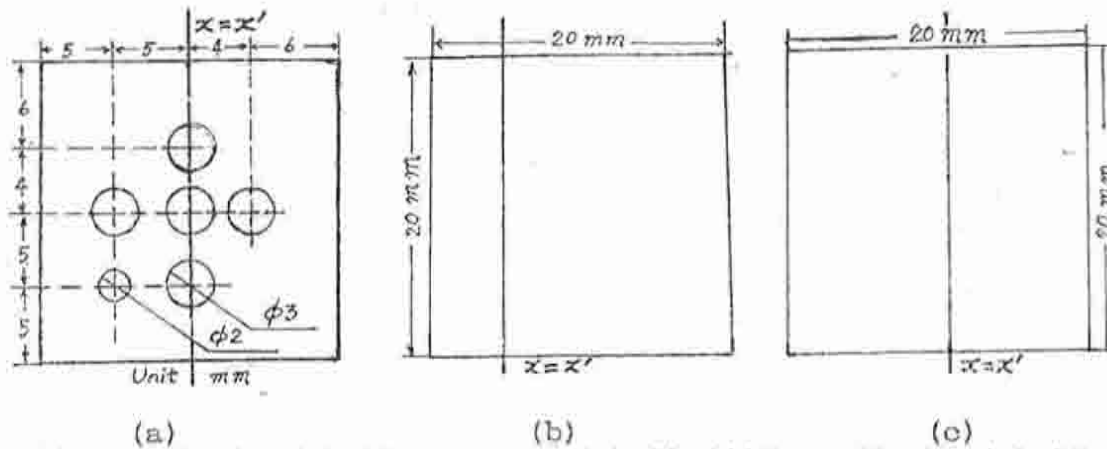


Fig.6 (a) Phantom with six holes (made of 4% agar aqueous solution), (b) and (c) Phantoms with no holes (made of 4% and 8% agar aqueous solution respectively)

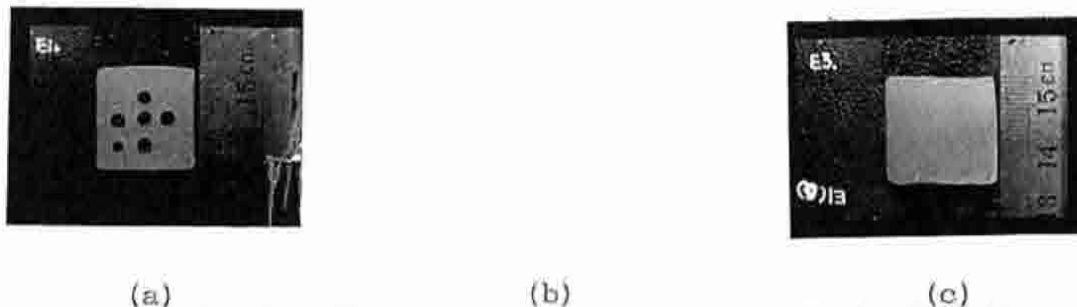


Fig.7 (a), (b) and (c) Photographs of the phantoms corresponding to Fig.6 (a), (b) and (c) respectively

VI. EXPERIMENTAL RESULTS

Fig.8 (a), (b) and (c) are the images of the B-scanner and are corresponding to Fig.7 (a), (b) and (c) respectively. It can be seen from these images that only the outlines of the internal structures of the testing objects are provided. Fig.9 (a), (b) and (c) are the images reconstructed by the QRI method from the phantoms shown in Fig.7 (a), (b) and (c) respectively.

Fig.10 (a), (b) and (c) are the comparisons of the reconstructed values (real lines) of the images in Fig.9 and the real values (dashed lines) on the lines $x = x'$ shown in Fig.6 (a), (b) and (c), respectively. From Fig.8, Fig.9 and Fig.10, one can see that the images reconstructed by QRI method are quantitative and are more helpful in understanding the internal structures of the testing objects than the B-scan images.

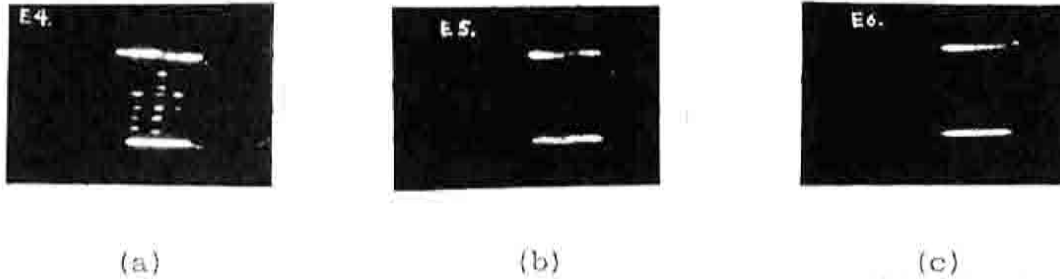


Fig.8 (a), (b) and (c) are the images obtained by the B-scanner and are corresponding to Fig.7 (a), (b) and (c) respectively

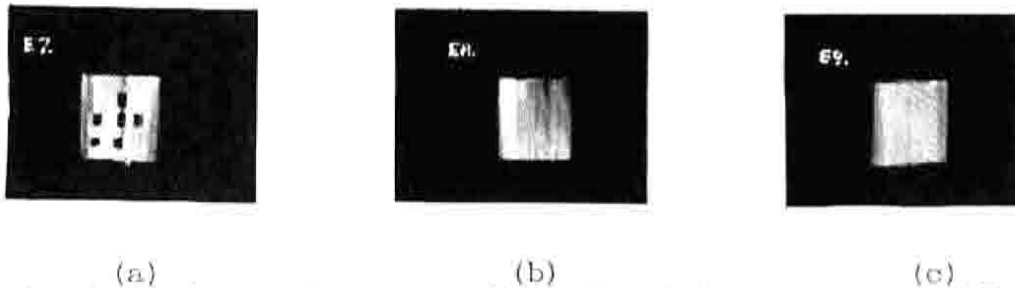


Fig.9 (a), (b) and (c) are the images reconstructed by the QRI method and are corresponding to Fig.7 (a), (b) and (c) respectively

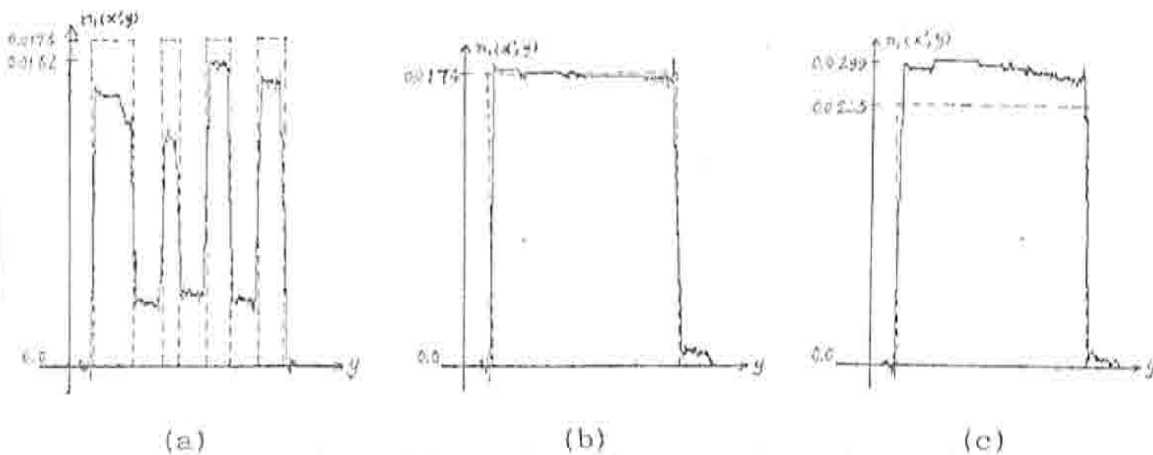


Fig.10 (a), (b) and (c) are the figures of the comparisons of the reconstructed values (real lines) of the images in Fig.9 and the real values (dashed lines) on the lines $x = x'$ shown in Fig.6 (a), (b) and (c) respectively

VII. SUMMARY

1. An experimental system for the QRI method is built up in this paper and the practical images of the testing objects are reconstructed using the data obtained from this system.

2. The experimental results show that (1) the images reconstructed by the QRI method are quantitative and (2) the images reconstructed by the QRI method are more helpful in understanding the internal structures of the testing objects than those obtained by the B-scanner.

3. From the experimental studies above, one can observe that the QRI method will be useful in tissue characterization and will enhance the ability of the B-scanner for diagnosing diseases, and it is shown that a substantial progress in obtaining ultrasonic diagnostic images is made.

VIII. REFERENCES

1. Jian-Yu Lu and Yu Wei, "A New Method for Quantitative Reflection Imaging", in Acoustical Imaging, Vol.17, Edited by Dr. Jun-ichi Kushibiki, 1988 (17th International Symposium on Acoustical Imaging, Sendai, Japan, May 31-June 2, 1988)
2. Jian-Yu Lu, "A Study of Diffraction Tomography and Quantitative Reflection Imaging Method", dissertation for Ph.D degree, Southeast University, Nanjing, China, 1988